BioMedical Engineering OnLine

RESEARCH

Open Access

In vivo imaging of adipose-derived stem cell sheets on biodegradable nonwoven fabric using X-ray CT

Hiroshi Sunami[1*], Yusuke Shimizu[2,3], Hitoshi Nakasone[3], Naoko Futenma[3], Junko Denda[1], Sayaka Yokota[3], Hidehiro Kishimoto[2], Masashi Makita[4] and Yasutoshi Nishikawa[4]

*Correspondence:
sunami@med.u-ryukyu.ac.jp

[1] Faculty of Medicine, University of the Ryukyus, Nishihara-cho, Japan
[2] Graduate School of Medicine, University of the Ryukyus, Nishihara-cho, Japan
[3] University of the Ryukyus Hospital, Nishihara-cho, Japan
[4] ORTHOREBIRTH Co., Ltd., Yokohama, Japan

Abstract

Background: A biodegradable nonwoven fabric that can be used to extract adipose-derived stem cells (ADSCs) from adipose tissue slices was developed, which were cultured rapidly without enzymatic treatment. The extracted and cultured ADSCs remain on the nonwoven fabric and form a thick cell sheet. The aim was to use the thick cell sheet as a treatment by transplanting it into the living body. In addition, the expectation was that it will be possible to observe the cell sheet in the living body using X-ray computed tomography (CT) because the nonwoven fabric used to produce the cell sheet contains 50% (by weight) hydroxyapatite.

Results: Thick cell sheets of ADSCs supported by two layers of nonwoven fabric were cut to size and transplanted into the cheeks of rats. No health damage was observed in the rats in which the cell sheets were implanted, except for one in which the surgery appeared to have failed. X-ray CT imaging showed that the fabric of the implanted cell sheet biodegraded over 12 weeks. Changes in the position, shape, and size of the cell sheet within the rat's body were tracked by X-ray CT. The thick cell sheets, which can be easily produced by simply seeding tissue slices, can be cut into appropriate shapes and transplanted safely, and it was confirmed that they slowly biodegraded when transplanted into the rats' bodies.

Conclusions: We demonstrated not only that the thick ADSC sheets can be transplanted successfully into animals, but also that the transplanted sheets can be observed in vivo by X-ray CT, which also allows changes in the ADSC sheets to be tracked. The results suggest that the biodegradable nonwoven fabric will be a useful transplantation device to ensure cell engraftment throughout the affected area, and facilitate monitoring of the transplant's subsequent status. We expect that this transplantation device will promote the development of regenerative therapy.

Keywords: Cell culture scaffold, Fiber structure, Transplantation device, PLGA

Introduction

Cell therapy, in which adipose-derived stem cells (ADSCs) are transplanted into the whole body or affected areas, is being actively implemented [1]. In ADSC therapy, transplantation of ADSCs as a cell suspension and as a cell sheet are both being actively studied. However, as will be described later, this cell therapy is subject to problems, including the high cost of cell preparation [2–4], difficulty in treating large affected areas [1, 4–6], and difficulty in engrafting cells into the affected area for a long period of time [7–13]. To solve these problems, we developed our own adipose-derived stem cell sheet (ADSC sheet), and aim to use it in clinical applications [4].

A biodegradable nonwoven fabric was used to fabricate the ADSC sheet. Nonwoven fabrics made from biodegradable polymers, or nonwoven fabrics made from biopolymers, are biodegradable and decompose slowly in a living body. Therefore, the suitability of biodegradable nonwoven fabrics as a scaffold for transplantation into living body organisms has been studied for a long time [4, 14–26, 44]. Such fabrics have been transplanted directly into animals [18, 20–23], or after seeding with cells in vitro to generate a cell sheet [14, 19, 24–26, 44]. Although non-biodegradable nonwoven fabrics have also been studied extensively, they are used mainly to develop three-dimensional culture techniques in vitro [27–33]. Studies show that ADSCs can be extracted from adipose tissue using a non-biodegradable nonwoven fabric [34, 35]; indeed, we extracted ADSCs successfully from adipose tissue using biodegradable nonwoven fabric, followed by culture to generate and ADSC sheets [4]. This technique involves extracting ADSCs from adipose tissue slices and rapidly culturing them without enzymatic treatment using a biodegradable nonwoven fabric. A critical feature of this system is that the fabric is made from materials already approved for use in medical devices: a biodegradable polymer poly(lactic-*co*-glycolic acid) (PLGA), and hydroxyapatite (HAp). This nonwoven fabric has a high affinity for adipose tissue and ADSCs, and can be used as a scaffold to quickly produce large numbers of ADSCs within a small volume. The high anisotropy of the fibers in the nonwoven fabric facilitates rapid extraction and proliferation of ADSCs [4]. In addition, the density of ADSCs increases more rapidly if they are extracted from adipose tissue slices and cultured on the nonwoven fabric in a culture vessel to which the cells do not adhere strongly [4]. The term "Extraction" rather than "Separation" is used in this study because the ADSCs on a nonwoven fabric are not separated from a cell population; rather, they are extracted from the tissue by the nonwoven fabric.

The new system was developed to solve three problems faced in the use of ADSCs in regenerative medicine. The first is that production of ADSCs is costly [2–4]. The second is the difficulty in filling a tissue volume with cells when the affected part is deformed or large [1, 4–6]. The third is the difficulty in ensuring that injected cells are targeted accurately and remain viable for long periods of time [7–13]. These challenges are relevant to a variety of therapies, and must be addressed for regenerative medicine to be successfully implemented. The system described above is expected to address these three problems. The cost of producing ADSCs from adipose tissue can be significantly reduced using a nonwoven fabric to eliminate the need for the enzymatic treatment typically used to disperse adipose tissue, and the need for passaging the cells. Use of the nonwoven fabric also reduces the space required for cell culture. In addition, if the nonwoven fabric is used as a filler for large anatomical regions of variable shape, it might be

possible to fill the affected areas. Finally, ADSC sheets growing on the nonwoven fabric are expected to engraft readily after transplantation and to remain in the vicinity of the affected areas for long periods of time because the ADSCs adhere firmly to the scaffold at the time of transplantation. Although there have been previous reports of adipose tissue slices with ADSCs seeded onto nonwoven fabric [34, 35], the material used here can be implanted directly into tissue in vivo because it consists entirely of biodegradable polymers approved for medical devices. Here, we aim to use ADSC sheets fabricated using the new system for the cell sheet transplants. For this purpose, it is necessary to transplant the cell sheet into animals and test whether any problems occur.

In this study, we succeeded in fabricating ADSC sheets by seeding and culturing adipose tissue slices between two layers of nonwoven fabric, and demonstrate that these ADSC sheets can be successfully transplanted into rats. We cut the cell sheet to a size and shape appropriate for the affected area at the time of transplantation. Moreover, we also tracked in vivo changes in the transplanted sheet using X-ray computed tomography (CT). Through these methods, we will evaluate the effectiveness of adjusting the size and shape of the cell sheet according to the size and shape of the affected area, as well as the ability to accurately engraft therapeutic cells to the affected area and retain them there for a long period of time. Furthermore, we confirmed biodegradation of the implanted fabric and the safety of the procedure. We would like to use the sheet not only for ADSCs, but also for other cell types for regenerative therapy, and we therefore also investigated the fabrication of sheets of various cell types by inducing differentiation of ADSCs in the ADSC sheet into other cell types.

Results and discussion

Observation, analysis, and evaluation of the structure of the nonwoven fabric

The structure of the nonwoven fabric (23-mm diameter, Type A) (ORTHOREBIRTH, Japan) used in this study and the results of confocal laser scanning microscopy (CLSM) observations, image analysis, and structural parameter evaluation are described elsewhere [4]. An important characteristic of this nonwoven fabric is the high anisotropy that results from the alignment of its fibers, which facilitates rapid extraction and proliferation of ADSCs [4]. In the present study, a digital camera (Fig. 1a) and field emission-type scanning electron microscopy (FE-SEM) images (Fig. 1b) showed that the fibers were largely aligned throughout the fabric. Furthermore, observation of the FE-SEM

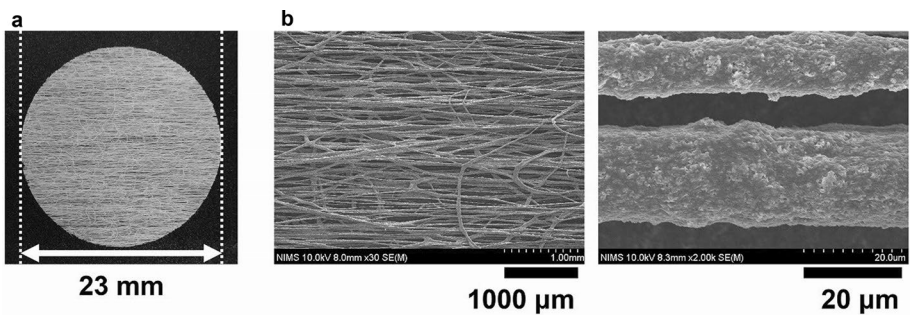

Fig. 1 Structure of the nonwoven fabric (23-mm diameter, Type A). **a** Digital camera image of the nonwoven fabric, **b** field emission-type scanning electron microscopy images of the nonwoven fabric

images (Fig. 1b) revealed that the fiber surfaces of the nonwoven fabric had irregularities of 1–2 μm, and that small pores with a diameter of 500 nm or less were present at intervals. After culturing, scanning electron microscopy (SEM) images were obtained and confirmed that the size of the small pores on the fiber surface had increased (Fig. 2). To assess changes in size, FE-SEM images of nonwoven fabric fibers before cell culture (Additional file 1: Fig. S3a, b) were compared with those after cell culture (Additional file 1: Fig. S3c, d). The pore area, pore ratio, and pore density on the surface of the fabric were determined to examine any significant differences between the values obtained before and after cell culture. The data revealed that the pore area after cell culture was greater than that before cell culture (Fig. 2c). In addition, the pore ratio after cell culture was higher than that before cell culture (Fig. 2d). By contrast, there was no significant difference in pore density (Fig. 2e). These results suggest that the use of nonwoven fabrics for cell culture results in both an increase in the size and proportion of pores on the fiber surface; however, the number of pores does not increase. We considered that these changes are the result of fiber decomposition.

There were small pores on the fiber surface after culture, and granule-like substances were visible inside the pores (Fig. 2a). We speculate that the granular substances contain hydroxyapatite because when fibers were generated without hydroxyapatite, these

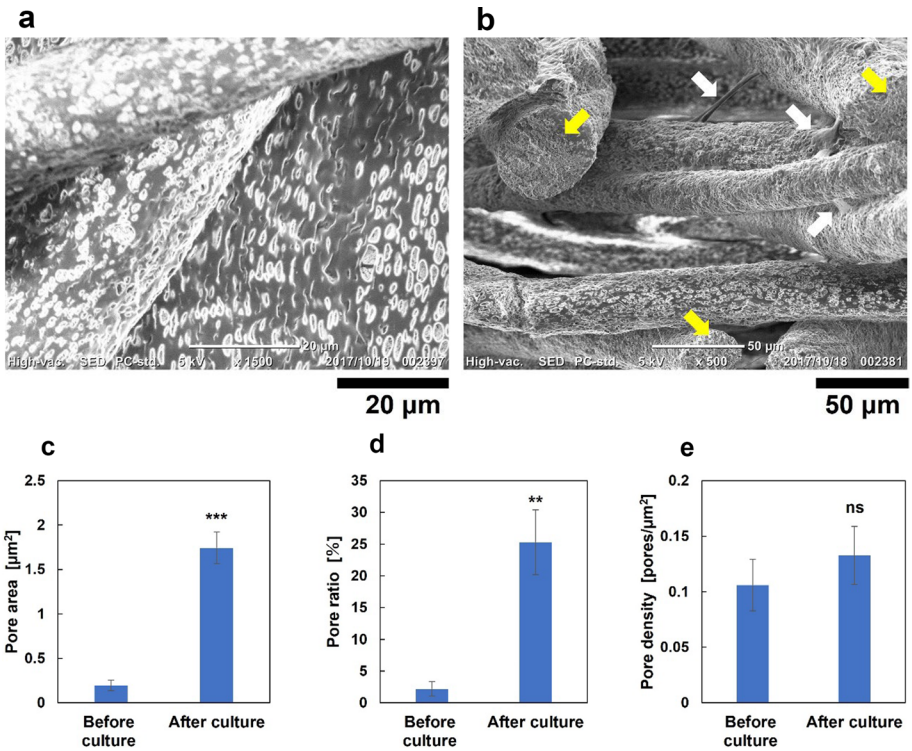

Fig. 2 SEM images of the nonwoven fabric fibers used for cell culture. **a** Magnified SEM image of the fiber surface. **b** SEM image of the fibers, along with the cross-sectional surface. To observe the surface of the nonwoven fabric, areas without cells were selected and imaged. The fine granules present in both SEM images are thought to be hydroxyapatite particles that were uniformly distributed within the fibers. Yellow arrows indicate the cross section. White arrows indicate cell protrusions. **c** Comparison of the pore area before and after cell culture. **d** Pore ratio after cell culture compared with that before cell culture. **e** Pore density after cell culture compared with that before cell culture

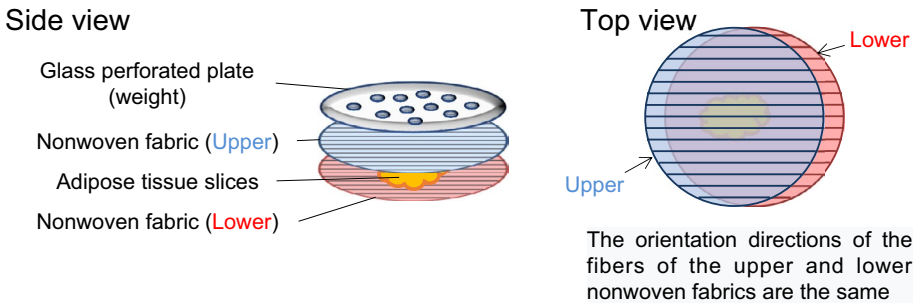

Fig. 3 Schematic illustration of adipose tissue slices seeded to nonwoven fabrics. The method for seeding the adipose tissue slices for extracting and culturing ADSCs on nonwoven fabric is represented. The straight lines drawn on the nonwoven fabric indicate the orientation of the fibers

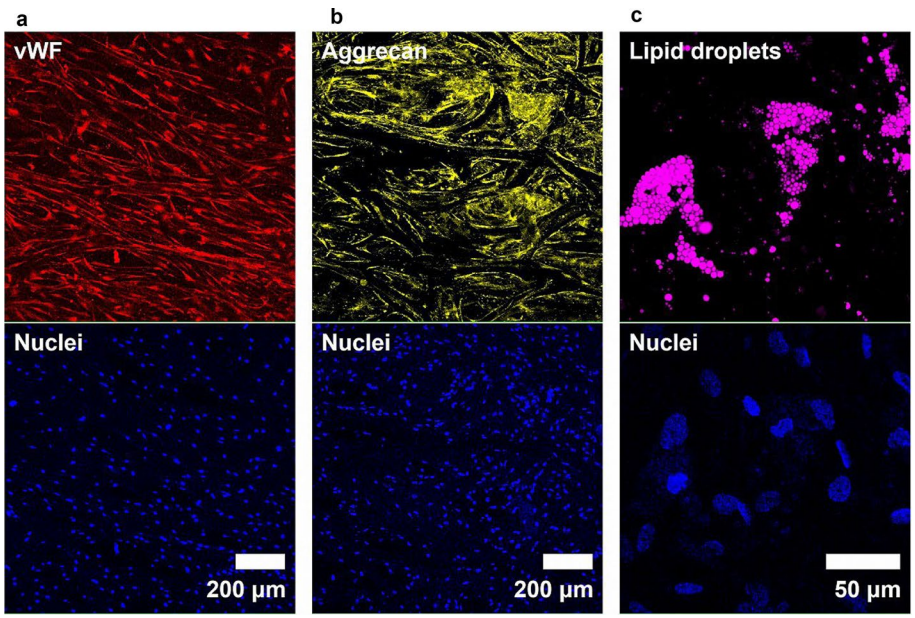

Fig. 4 CLSM images of cell sheets differentiated from ADSCs cultured on nonwoven fabric. **a** Cell sheet induced to differentiate into vascular endothelial-like cells. Red indicates von Willebrand Factor (vWF). **b** Cell sheet induced to differentiate into chondrocyte-like cells. Yellow indicates aggrecan. **c** Cell sheet induced to differentiate into adipocyte-like cells. Pink indicates lipid droplets. Blue in **a**, **b**, and **c** indicates cell nuclei

granules did not appear (data not shown). In the future, elemental mapping of the surface will be conducted using SEM–EDX to clarify whether the granules inside the pores contain highly concentrated hydroxyapatite. We also speculate that the small pore structure of the fibers greatly influences the decomposition rate of the nonwoven fabric.

Differentiation of ADSCs into vascular endothelial cells, chondrocytes, and adipocytes

After seeding (Fig. 3) and culturing the adipose tissue slices in ADSC–GM (Lonza, USA) for 3 or 40 days, ADSCs were extracted from the slices and induced to differentiate into vascular endothelial cells (Fig. 4a), chondrocytes (Fig. 4b), or adipocytes (Fig. 4c) during culture on the nonwoven fabric. CLSM images revealed expression of the molecular markers von Willebrand factor (vWF) for vascular endothelial cells, aggrecan for

chondrocytes, and lipid droplets for adipocytes. These results indicated that uninterrupted differentiation of ADSCs can be achieved by culturing adipose tissue slices on the nonwoven fabric, and that there was no need for enzymatic treatment, extraction, or passaging of the cells. In a previous study, ADSCs were extracted and cultured from adipose tissue seeded onto nonwoven fabric for 34 days, and flow cytometry analysis confirmed the high purity of the ADSCs [4]. In the present study, the majority of the cells extracted from adipose tissue slices and cultured on the nonwoven fabric were induced to differentiate into various types of cells, supporting that the cells extracted and cultured from the adipose tissue slices were also highly pure ADSCs. Since the ADSCs differentiated into vascular endothelial cell-like, chondrocyte-like, and adipocyte-like cells, it is assumed that they maintained multipotency. In future studies, we will perform western blotting and PCR analysis of marker proteins to further evaluate the differentiation state of ADSCs induced to differentiate. This type of cell sheet should improve the safety, quality, and cost performance of regenerative therapy for various organs and tissues. The endothelial cell sheets should be particularly useful because blood vessels are indispensable for all organs and tissues.

ADSC sheets sandwiched between nonwoven fabrics and transplanted into rats

The ADSC sheets used for transplantation were cultured (Fig. 3) for 30 days for safety assessment tests, and for 24 days for X-ray CT observations. The difference in the culture period of the ADSC sheets between the two experiments is down to matters of convenience for the experimental facilities.

The nonwoven fabric-supported ADSC sheets were cut into 10-mm squares and transplanted into the left cheeks of three F344/N Jcl-rnu/rnu rats and three Wistar rats (Fig. 5a). The six rats were used to establish the transplantation procedure and post-transplantation housing method. At the same time, the toxicity and safety of post-transplantation breeding were also studied. F344/N Jcl-rnu/rnu rats are athymic rats, and were used mainly as an immune-deficient model because they show a suppressed immune response, thereby allowing transplantation of human ADSC sheets. For comparison, the Wistar rats were used as controls for the F344/N Jcl-rnu/rnu rats, because Wister rats with normal immunity are used in a wide variety of studies for toxicity and safety testing.

(See figure on next page.)

Fig. 5 Transplantation of cell sheets into animals. **a** Two-layer ADSC sheet cut into a 10-mm square was transplanted into the left cheek of a Wistar rat. **b** Scanning electron microscopy image of an ADSC sheet prepared on the nonwoven fabric. The sample preparation and observation methods were the same as those in Fig. 2. **c** 3D X-ray CT image of a rat's left face. The inhalation port for inhalation anesthesia was enlarged to accommodate growth of the rat (outer diameter = 2 cm before and 1 week after transplantation, and 3.4 cm after 12 weeks). Red arrows indicate cell sheets. **d** Segmentations of a 3D region of each X-ray CT image of the cell sheet supported by two layers of the nonwoven fabric. The X-ray CT images were captured for 12 weeks. Only images from week 5 to week 11 were captured every other week. All others (from week 1 to week 5 and from week 11 to week 12) were captured every week. The segmented images are posterior views of one cell sheet transplanted into a F344/N Jcl-rnu/rnu rat. **e** Volume change of the transplanted cell sheets in F344/N Jcl-rnu/rnu rats, as estimated from CT images ($n = 5$). Statistical significance tests (Dunnett) were performed using week 1 as the control. Combinations showing a significant difference are marked by an asterisk. Statistical data and p values are presented in Additional file 1: Table S1

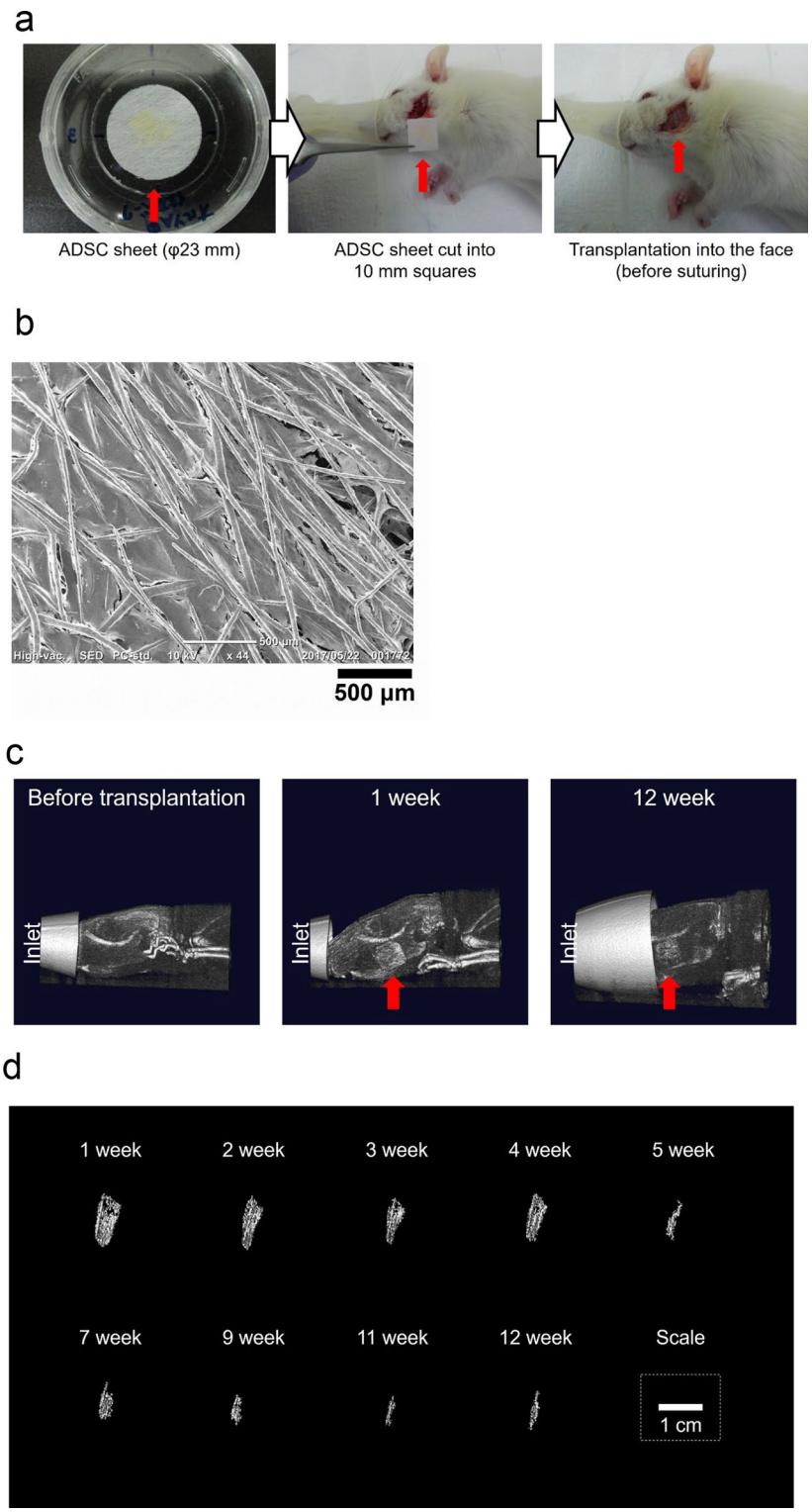

Fig. 5 (See legend on previous page.)

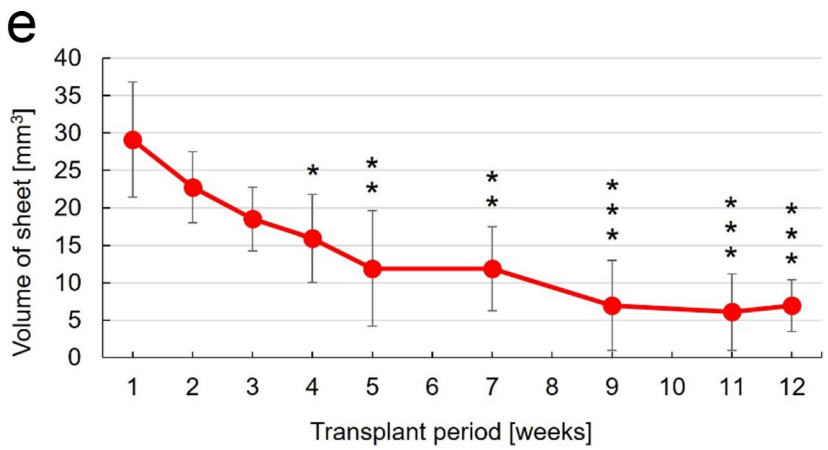

Fig. 5 continued

The ADSC sheets could be easily cut into 10-mm squares with scissors, and the cut ADSC sheets maintained their shape and did not collapse or wrinkle, even when pinched with tweezers (Fig. 5a). Moreover, their shape was maintained even when subcutaneously implanted, which supports their utility as a subcutaneous implantation device. One of the F344/N Jcl-rnu/rnu rats immediately began to accumulate fluid at the transplant site and died 4 weeks later, which may have been the result of a problem during surgery, but could also have been due to the conventional experimental environment, rather than the use of a specific pathogen-free environment. The two remaining F344/N Jcl-rnu/rnu rats survived for 6 months after transplantation. One of the three Wistar rats survived for 6 months after transplantation, while the other two survived for more than 18 months. Except for the one death, none of the rats developed abnormalities such as inflammation or deformities at the transplantation site. The two nude rats (F344/N Jcl-rnu/rnu rats) transplanted with the human ADSCs sheet survived for 6 months, which is shorter than the natural lifespan of the rats; however, the conventional environment used for transplantation and rearing can be particularly harsh on nude rats, which in general have poor immune functions [36]. It is thought that safety is not an issue because the two nude rats survived for 6 month post-transplantation in such a harsh environment, with no adverse effects at the transplantation site. Furthermore, none of the Wister rats (which have normal immune functions) developed abnormalities at the transplantation site, and all survived for more than 6 months. Therefore, transplantation with the human ADSCs sheet exhibited no toxic effects and raised no safety concerns. The reason for transplanting and rearing the rats under conventional environmental conditions rather than under specific pathogen-free (SPF) conditions is that transplantation and X-ray CT scanning of ADSC sheets at the Institute for Animal Experiments of University of the Ryukyus can only be performed under conventional environmental conditions. Once rats are placed in the conventional environmental conditions for transplantation or X-ray CT scanning, they cannot be returned to the SPF conditions.

In addition, we transplanted ADSC sheets cut into 10-mm squares into five F344/N Jcl-rnu/rnu rats and evaluated changes in sheet volume using X-ray CT images. HAp mixed with the nonwoven fibers at a weight fraction of about 50% contributed greatly to image contrast enhancement. The fine granules in the left and right SEM images (Fig. 2)

are assumed to be hydroxyapatite particles, and it can be seen that they were uniformly distributed. SEM imaging of ADSC sheets showed that cells filled the spaces between fibers in the nonwoven fabric (Fig. 5b), indicating that the volume of the nonwoven fabric on the X-ray CT images approximated that of the cell sheet. The X-ray CT images revealed the position and approximate shape of the cell sheet (Fig. 5c) after transplantation. In Fig. 5c, a 10-mm square sheet can be clearly seen on the left face of the rat after 1 week, while the sheet is less visible after 12 weeks. To analyze cell sheet volume, a 3D region of the cell sheet supported by two nonwoven fabric layers was segmented from each X-ray CT image (Fig. 5d and Additional file 1: Fig. S1). Changes in the cell sheet volume in the X-ray CT images acquired from the 1st to 12th week after transplantation are shown in Fig. 5e. The cell sheet volumes after the 4th week were significantly lower than the first week, demonstrating that remarkable decomposition of the transplanted ADSC sheets had occurred between first week and 4th week after transplantation. The X-ray CT image volume of the transplanted sheet at the 12th week was less than 24% of that at the first week. We consider the 44 mm^3 outer volume of the cell sheet before transplantation to be different from the 29 mm^3 volume estimated from the CT image at the first week following transplantation, when there was very little biodegradation of the nonwoven fabric. This is because the nonwoven fabric used as the scaffold for the cell sheet has many voids, as shown in Fig. 1b and Fig. 2b, which result in the volume of the cell sheet obtained from the X-ray CT images being smaller than the outer volume. It should be noted that the cell sheet outer volume of 44 mm^3 ($0.44 \times 10 \times 10$ mm) was calculated with reference to the average 0.22-mm thickness of the nonwoven fabric [4]. These results show that the position, shape, and volume changes of cell sheets fabricated on nonwoven fabric containing 50% HAp by weight can be easily tracked by X-ray CT imaging after transplantation. The ability to track changes in these cell sheets in vivo after transplantation has the potential to greatly increase the efficiency of regenerative therapy research.

However, the nonwoven fabric supporting the cell sheet is a foreign substance; therefore, it is desirable that such artificial scaffolds disappear after treatment is completed. It is for this reason that biodegradable scaffolds are attracting a lot of attention. To make the most of this advantage, it would be appropriate to adjust the size of the scaffold so that it disappears at the end of treatment. We believe that cell sheets or biodegradable nonwoven fabrics observable by X-ray CT are extremely useful for optimizing the period of biodegradation in vivo.

In the future, we would like to remove the transplanted cell sheets to directly evaluate their volume and structure, as well as the cellular and extracellular matrix composition. If the transplanted sheets are removed from the body, and the actual volume is measured and compared with that calculated from the X-ray CT image, the correlation can be clarified. In future, we will be able to predict changes in the volume of the cell sheet from the X-ray CT images alone.

The cell sheets supported on this type of nonwoven fabric can range in size from that of a coin to an A4 sheet of paper [4], and can be shaped to fit the affected area, as shown in Fig. 5a. It is also possible to treat larger volumes by folding or rolling the sheets to increase thickness. We were also able to create softer nonwoven fabrics and nonwoven fabrics, which are easier to roll into a cylindrical shape, by adjusting only the spinning

method; no changes to the material composition were required (data not shown). In future, we would like to prepare nonwoven fabrics with appropriate stiffness for transplantation at various sites. We are therefore confident that this nonwoven fabric will be useful in regenerative medicine as a device facilitating reliable placement and retention of stem cells for long periods throughout the affected area.

Conclusion

In this study, we report that ADSC sheets made by sandwiching adipose tissue slices between layers of biodegradable nonwoven fabric can be successfully transplanted into animals. To our knowledge, this is the first time that a cell sheet prepared by directly seeding tissue slices onto a scaffold has been transplanted into a living body. It was also confirmed that the cell sheet also has the great advantage that its state can be tracked in vivo using X-ray CT imaging. Moreover, we report that not only is it possible to easily extract and culture ADSC sheets on the nonwoven fabric, but that they can also be induced to undergo uninterrupted differentiation into sheets of vascular endothelial-, chondrocyte-, and adipocyte-like cells. It will be important to confirm the therapeutic effects of these cell sheets by transplanting them as stem or differentiated cells into various tissues and animal models of disease. We have also formed cell sheets by seeding and culturing many other types of cells and tissues on this nonwoven fabric, and plan to evaluate their use in regenerative therapies in the future.

Materials and methods

Preparation of biodegradable nonwoven fabric

The fibers that made up the nonwoven fabric comprised the biodegradable polymer PLGA, to which hydroxyapatite (Hap) was added (weight ratio, 1:1) to increase adhesion of the cells to the fibers. Since PLGA-only nonwoven fabrics have a low cell adhesion ability (data not shown), hydroxyapatite was added to improve cell adhesion. Furthermore, to develop a nonwoven fabric that can be imaged more clearly using X-ray CT, the hydroxyapatite content of the fibers making up the nonwoven fabric can be increased. The decision to use a hydroxyapatite content of 50% by weight was made because 50% is the limit at which the desired fiber could be spun in a stable manner. The PLGA used was LG855S (inherent viscosity 2.5–3.5 dL/g, Evonik Industries AG, Germany). HAp was a special-order product made by Taihei Chemical Industrial (Japan). Many of the scaffolds containing HAp that have been used for culturing ADSCs can also be used to induce their differentiation into vascular endothelial- [37–40], chondrocyte- [34, 41], osteoblast- [37–39, 42–47], and adipocyte-like cells [48]. A composite solution was prepared by uniformly mixing HAp particles with PLGA dissolved in a solvent, from which nanofibers were spun using a NANON-3 electrospinning device (MECC, Japan). All raw materials and solvents were approved for medical devices.

The nonwoven fabric was fabricated by depositing a fiber on the surface of the NANON-3 rotary drum. It is possible to manufacture large-area nonwoven fabric by reciprocating the nozzle that sprays the spinning solution onto the rotating drum. Many types of nonwoven fabric with different structures have been fabricated by changing the manufacturing conditions of the nonwoven fabric [4]. Here, only Type A nonwoven fabric was used because it was the most effective for extraction and culture of ADSCs from

adipose tissue slices [4]. After spinning, the nonwoven fabric wrapped around the drum was cut into a rectangle, placed on a flat table, and formed into a circle using a hollow mold. The biodegradable nonwoven fabric was produced by ORTHOREBIRTH (Japan), and sterilized by gamma irradiation. More detailed information about its fabrication was provided previously [4].

Imaging of the nonwoven fabric

Macroscopic images of the nonwoven fabric were captured by a Power Shot SX210 IS digital camera (Canon, Japan; Fig. 1a). Microscopic images of the nonwoven fabric were captured by an FE-SEM SU3500 (Hitachi, Japan; Fig. 1b). The nonwoven fabric used for FE-SEM observation was platinum coated (350 Å) with an IB-5 ion coater (Eiko, Japan).

SEM observation of cell sheets

SEM images of the nonwoven fabric fibers used for cell culture were acquired (Fig. 2a, b). ADSCs (PT-5006, Lonza, USA) were seeded onto the nonwoven fabric at 3.0×10^4 cells/cm^2. The cell sheets were prepared by culture in ADSC–GM for 20 days before fixation with 4% paraformaldehyde in phosphate buffered saline (PBS; Nacalai Tesque, Japan) overnight at room temperature, followed by washing once with D-PBS (Nacalai Tesque, Japan) and once with Milli-Q grade water. After washing, the cell sheet was placed on conductive copper foil on double-sided tape (Teraoka Seisakusho, Japan) on a removable SEM sample stage and air-dried for at least 2 weeks. After coating the dried cell sheet with platinum, the samples were observed with an SEM (JCM-6000, JEOL, Japan).

Analysis of changes in surface pores after culture

The pore area (area per pore), pore ratio (pore area/total area), and pore density (number of pores per unit area) on the surface of the nonwoven fabric were compared before and after cell culture. Two FE-SEM images (Additional file 1: Fig. S3a, b), taken using the method described above, were used to analyze the surface of the nonwoven fabric before cell culture, and two SEM images (Additional file 1: Fig. S3c, d) were taken to analyze the surface of the nonwoven fabric after cell culture. For each of these images, pores present in two 15 μm × 25 μm regions (measurement fields) were extracted by setting a threshold for image binarization; the average pore area, average pore ratio, and average pore density were then measured and analyzed ($n=4$). Pore extraction, measurement, and analysis were performed using Image Pro 10 (Media Cybernetics, USA). The pores to be extracted, measured, and analyzed were defined as those with deep bottoms that were not visible, or pores with raised edges and containing visible granular particles. The calculation for the average pore area included only pores for which the entire pore area sat completely within the measured region. The average pore ratio was calculated using all concave areas within a measured region as a total pore area, even if the pores were not completely within the measured region. The average pore density was calculated using the pores whose center was within a measured region.

Collection and bacteriostatic treatment of adipose tissue

The study protocol (approval number 810) was approved by the Ethics Committee of the University of the Ryukyus for Medical and Health Research Involving Human Subjects,

and human adipose tissue was collected at the University of the Ryukyus Hospital. Informed written consent was obtained from all human subjects who donated adipose tissue. The adipose tissues used in this study were collected from donors (i)–(iii) by liposuction (Table 1). Bacteriostatic treatment and washing were performed to reduce the risk of contamination. After collection, each adipose tissue sample was immediately soaked in perfusion solution (Merk, Germany) with 1% penicillin G potassium (Meiji Seika Pharma, Japan) and cleaned by centrifugation (800 G, 5 min, 4 °C). After cleaning, we transferred the adipose tissue to a new 50 mL centrifuge tube containing perfusion solution with 1% penicillin G potassium and treated the tissue bacteriostatically by allowing it to stand at 4 °C overnight. Personal experience suggests that the frequency of contamination is greatly reduced when such a bacteriostatic treatment is performed. After the bacteriostatic treatment, we washed the tissue three times by centrifugation (800 G, 5 min, 4 °C).

Preparation of the adipose tissue slices for seeding on the nonwoven fabric

Adipose tissue that had been treated bacteriostatically and washed was cut with sterilized scissors into slices of about 0.5–3 mm, and if necessary, torn with sterilized tweezers.

Degassing of the nonwoven fabric

The biodegradable circular nonwoven fabric was submerged into 10 mL of ADSC–GM in a 100-mm cell culture dish (Corning Inc., USA). A perforated glass plate (round, diameter 20 mm, thickness 3.0 mm, 1.9 g; Toshin Riko, Japan) was placed on each nonwoven fabric piece to prevent it from floating. The fabric was then degassed under reduced pressure (0.09 MPa, 1 min) using a water flow aspirator, as described previously [4, 49–51].

Seeding of adipose tissue slices on the nonwoven fabric

First, two sheets of the degassed 23-mm diameter circular nonwoven fabric (ORTHOREBIRTH, Japan) were placed on top of each other in a cell strainer placed into each well of a Costar® ultra-low attachment-surface 6-well plate (Corning Inc., USA) containing 4.5 mL ADSC–GM. A sterilized perforated glass plate (round, diameter 20 mm, thickness 3.0 mm, 1.9 g) was used as a weight on top of the two layers of nonwoven fabric. It is worth noting that Teflon perforated plates would have been preferable to glass perforated plates because cells adhere poorly to Teflon, whereas they adhere strongly to glass [4]. Then, 0.02 g slices or 0.05 g slices of adipose tissue were sandwiched between the two

Table 1 Anonymized information about the human tissue donors

Case	Date	Age, year/sex	Technique	Part	Height, cm	Weight, kg	BMI
(i)	Jul 9, 2018	54/F	Liposuction	Left thigh (superficial layer inside)	143.7	61.1	29.60
(ii)	Nov 26, 2018	26/F	Liposuction	Both lateral region of abdomen	149.8	51.3	22.90
(iii)	Sep 18, 2019	56/F	Liposuction	Abdomen	157.0	56.0	23.04

layers of fabric, held down by the glass plate (Fig. 3), and started culturing at 37 °C/5% CO_2. Fibers were oriented in the same direction in the two nonwoven fabric layers.

Differentiation of ADSCs in the tissue sheets

The ADSCs in the tissue sheets (prepared from adipose tissue slices) were differentiated into vascular endothelial cells, chondrocytes, or adipocytes. The adipose tissue slices used in this experiment were prepared by sandwiching 0.02 g slices of adipose tissue from case ii (Table 1) between two layers of fabric, holding them down with a glass plate (Fig. 3), and culturing them at 37 °C/5% CO_2. These samples were then used for each of the following experiments.

First, cells were differentiated into vascular endothelial cells. Briefly, after seeding and culturing the tissue slices in ADSC–GM for 3 days, differentiation into vascular endothelial cells was induced by changing the medium to EGM-2 (Lonza, USA); this medium was then replaced with fresh medium every 3 days for 32 days [52, 53]. After induction of differentiation, the samples were fixed in 4% paraformaldehyde in PBS and labeled with a vWF rabbit host antibody (Sigma-Aldrich, USA; 1:100, 4 h) followed by Alexa Fluor 546 goat anti-rabbit IgG (Thermo Fisher Scientific Inc., USA; 1:200, 4 h). The samples were then stained with DAPI (Fujifilm Wako Chemicals, Japan; 1:400, 20 min). Two binder clips were placed on the edges of the nonwoven fabric to prevent it from moving, and each nonwoven fabric sample was placed seeded side up into a 35-mm cell culture dish (Corning Inc., USA) containing D-PBS. Samples were observed by upright CLSM (FV1000D, Olympus, Japan) fitted with a water-immersion objective lens (UMPLFLN 10×W; Olympus, Japan). A total of 101 images of area 1270 μm × 1270 μm at intervals of 3.0 μm were observed in the Z-axis direction to ensure that the entire thickness from the top surface (in the case of an upright microscope, the surface close to the objective lens) to the bottom surface was captured (Fig. 4).

Next, the cells in the sheet were differentiated into chondrocytes. Briefly, after seeding and culturing the tissue slices for 40 days in ADSC–GM, differentiation into chondrocytes was induced by changing the medium to chondrocyte differentiation medium, which was then replaced with fresh medium every 3 days for 21 days. The chondrocyte differentiation medium used in this experiment was high-glucose Dulbecco's modified eagle medium (Nacalai Tesque, Inc., Japan) supplemented with 10% fetal bovine serum (Invitrogen, USA) and cartilage differentiation factors (0.04 mg/mL L-proline (Sigma-Aldrich, USA), 100 nM dexamethasone (Fujifilm Wako Chemicals, Japan), 1×ITS + 1 liquid media supplement (Sigma-Aldrich, USA), and 10 μg/mL TGF-β3 (Fujifilm Wako Chemicals, Japan)). The choice of these differentiation factors was based on several previous studies [54–57]. After induction of differentiation, the samples were fixed in 4% paraformaldehyde in PBS, washed three times with D-PBS containing 0.1% Tween 20 (Sigma-Aldrich, USA), and immersed for 3 h in D-PBS containing 3% BSA. The fixed samples were then reacted with an anti-aggrecan antibody (Abcam, UK; 1:200, overnight, 4 °C), followed by Alexa Fluor 546 goat anti-mouse IgG1 (Thermo Fisher Scientific Inc., USA; 1:400, 4 h), and then staining with DAPI (1:400, 20 min). After fluorescence staining, the samples were observed by CLSM FV1000D, as described above.

Finally, cells in the sheet were differentiated into adipocytes. Briefly, after seeding and culturing the tissue slices for 40 days in ADSC–GM, differentiation into adipocytes was

induced by changing the medium to adipocyte differentiation medium BBDM2 (Sumitomo Dainippon Pharma, Japan) and culturing for 7 days; in this case the medium was not changed during culture [58]. After induction of differentiation, the cells were cultured for 7 days in adipocyte maintenance medium BBAM1 (Sumitomo Dainippon Pharma, Japan) to allow accumulation of lipid droplets, which are a marker of adipocytes. The samples were then fixed in 4% paraformaldehyde in PBS and stained for with DAPI (1:400, 20 min) and Nile red (Fujifilm Wako Chemicals, Japan; 1 μg/ml, 40 min). The stained samples were then observed by CLSM FV1000D equipped with a water-immersion objective lens (UMPLFLN 60×W; Olympus, Japan). The samples were then placed in a culture dish for observation, as described above. A total of 101 images of area 212 μm × 212 μm at intervals of 3.0 μm were observed in the Z-axis direction to ensure that the entire thickness from the top surface (in the case of an upright microscope, the surface close to the objective lens) to the bottom surface was captured.

Culture of adipose tissue slices on the nonwoven fabric prior to transplantation

To assess the safety of the cell sheet transplantation method, a 0.05 g piece of adipose tissue slices was prepared from adipose tissue case i (Table 1), seeded, and cultured at 37 °C/5% CO_2 in ADSC–GM; the medium was replaced with fresh medium every 3 days for 30 days. To investigate changes in cell sheet volume using X-ray CT, a 0.05 g piece of adipose tissue slice was prepared from adipose tissue case iii (Table 1), seeded, and cultured at 37 °C/5% CO_2 in ADSC–GM; the medium was replaced with fresh medium every 3 days for 24 days.

Transplantation into animals

The aim of the animal experiments was to test whether the cell sheets supported on nonwoven fabric could be used for the treatment of facial nerve paralysis in an animal model. In this report, the safety of the cell sheet transplantation into the cheeks of a facial nerve paralysis rat model was evaluated, and CT was used to investigate changes in the volume of the cell sheets. Cell sheet transplantation into rats was considered safe if no abnormalities at the transplant site were observed, and if the rats survived for 6 months or more after transplantation. Although 6 months is shorter than the natural lifespan of a rat, this was selected as the guideline for safety assessment, considering that transplantation and rearing were carried out in a conventional (rather than SPF) environment. Transplantation and rearing in a conventional environment is extremely harsh for nude rats, which are usually maintained in an SPF environment [36]. In both studies, the cell sheets were supported on 23-mm-diameter circular nonwoven fabric prepared by a method similar to that described above, but for inducing differentiation. The sandwich culture described above, which consisted of two layers of fabric, was also used for transplantation into the animals. These animal experiments were approved by the Animal Care and Use Committee of the University of the Ryukyus (approval number: A2018041). Rat surgery and breeding were carried out in a conventional environment, rather than in a specific pathogen-free (SPF) environment. Animal breeding was carried out by the Institute for Animal Experiments of University of the Ryukyus. The therapeutic effect of the cell sheet for treatment of facial nerve paralysis was not investigated in this study because an evaluation method has not yet been developed.

Three 6-week-old male F344/N Jcl-rnu/rnu rats were purchased from Cler Japan (Japan) and three 6-week-old male Wistar rats were purchased from Charles River Laboratories Japan (Japan). After the rats were brought into the Institute for Animal Experiments of University of the Ryukyus and housed for 1 week to accustom them to the environment of the institute, cell sheets supported by the two layers of nonwoven fabric were transplanted into the 7-week-old rats. All transplantations were performed with the rats anesthetized by inhalation of isoflurane (introduction: 4%, sustainment: 2–3%). An all-in-one small animal anesthesia machine (MK-AT210D, Muromachi Kikai, Japan) was used for inhalation anesthesia. Before transplantation, the rats were subjected to facial diplegia by making incisions and cutting a facial nerve trunk on both sides; the success of the procedure was confirmed by the absence of whisker movement. On the left cheek, a cell sheet supported by two nonwoven fabric pieces cut into 10-mm squares was transplanted over the severed nerve and covered by sutured skin (Fig. 5a). The opposite cheek without transplanted tissue was used as a control. Observations were carried out for 12 weeks after transplantation.

To investigate changes in the volume of the cell sheets in F344/N Jcl-rnu/rnu rats, each rat was imaged by X-ray CT for 12 weeks. Only images from week 5 to week 11 were captured every other week. All others (from week 1 to week 5 and from week 11 to week 12) were captured every week. X-ray CT imaging was performed only on F344/N Jcl-rnu/rnu rats and not on Wistar rats. Because this cell sheet is a xenotransplant, it is desirable to evaluate it in F344/N Jcl-rnu/rnu rats, which are immunodeficient. Wistar rats were used only to establish the transplantation procedure and the post-transplantation housing method. It is important for the expansion of the use of this cell sheet that the transplantation procedure and post-transplantation housing method are established using Wister rats because Wister rats with normal immunity are used in a wide variety of studies. The X-ray CT imaging device used in this study was a 3D X-ray micro-CT R_mCT2 (Rigaku, Japan). This 3D X-ray micro-CT was operated using Database ver. 2.3.1.0 software (Rigaku, Japan). The 3D viewer function of the Database software was used to confirm the position and shape of the transplanted cell sheets (Fig. 5c). Analyze 12.0 software (Rigaku, Japan) was used to segment and measure a 3D region of the cell sheet supported by the two nonwoven fabric layers in each X-ray CT image (Fig. 5d and Additional file 1: Fig. S1). Analyze 12.0 was also used to identify the upper and lower limits of the reference threshold for each X-ray CT image (Additional file 1: Fig. S2). Using the reference threshold determined in the first week after transplantation, changes in the volume of the transplanted cell sheets were evaluated for 12 weeks (Fig. 5e).

Statistical analysis

All statistical analyses were performed using GraphPad Prism (GraphPad Software, Inc., USA). The results are expressed as mean ± standard deviation. Changes of the pore area, pore ratio, pore density in the fibers before and after culture were analyzed using Student's *t* test. Volume changes in the cell sheets after their transplantation into rats were analyzed using the one-way ANOVA with the Dunnett multiple comparisons test. $P < 0.05$ was considered significant. Ns, not significant; *, $p < 0.05$; **, $p < 0.01$;

***, $p < 0.001$. To ensure clear presentation of data, *, **, and *** are used to denote significance.

Supplementary Information

The online version contains supplementary material available at https://doi.org/10.1186/s12938-024-01324-x.

Additional file 1.

Acknowledgements
We thank University of the Ryukyus Center for Research Advancement and Collaboration for use of their facilities. A part of this work was supported by "Advanced Research Infrastructure for Materials and Nanotechnology in Japan (ARIM)" of the Ministry of Education, Culture, Sports, Science and Technology (MEXT). Proposal Number JPMXP1224NM0003.

Author contributions
The manuscript was written through contributions from all authors. All authors read and approved the final manuscript.

Funding
This work was supported by a grant from the Okinawa prefectural government through the Enterprise to Promote Practical Use of Advanced Medical Technology (Grant ID not available), JSPS KAKENHI Grant Number JP19H04448, JP19K09248.

Data availability
All the data are available within the manuscript.

Declarations

Consent for publication
All authors have agreed to submit the manuscript in its current form for consideration for publication in the Journal.

Competing interests
M. Makita and Y. Nishikawa work for ORTHOREBIRTH Co. Ltd., which sells products related to those in the present study.

Received: 11 May 2024 Accepted: 11 December 2024
Published online: 27 December 2024

References

1. Ntege EH, Sunami H, Shimizu Y. Advances in regenerative therapy: a review of the literature and future directions. Regenerat Ther. 2020;14:136–53.
2. Priya N, Sarcar S, Majumdar AS, SundarRaj S. Explant culture: a simple, reproducible, efficient and economic technique for isolation of mesenchymal stromal cells from human adipose tissue and lipoaspirate. J Tissue Eng Regen Med. 2014;8(9):706–16.
3. van Dongen JA, Tuin AJ, Spiekman M, Jansma J, van der Lei B, Harmsen MC. Comparison of intraoperative procedures for isolation of clinical grade stromal vascular fraction for regenerative purposes: a systematic review. J Tissue Eng Regen Med. 2018;12(1):e261–74.
4. Sunami H, Shimizu Y, Futenma N, Denda J, Nakasone H, Yokota S, Kishimoto H, Makita M, Nishikawa Y. Rapid stem cell extraction and culture device for regenerative therapy using biodegradable nonwoven fabrics with strongly oriented fibers. Adv Mater Interfaces. 2022. https://doi.org/10.1002/admi.202101776.
5. Rasmussen BS, Lykke Sorensen C, Vester-Glowinski PV, Herly M, Trojahn Kolle SF, Fischer-Nielsen A, Drzewiecki KT. Effect, feasibility, and clinical relevance of cell enrichment in large volume fat grafting: a systematic review. Aesthet Surg J. 2017;37(3):S46–58.
6. Wang C, Long X, Si L, Chen B, Zhang Y, Sun T, Zhang X, Zhao RC, Wang X. A pilot study on ex vivo expanded autologous adipose-derived stem cells of improving fat retention in localized scleroderma patients. Stem Cells Transl Med. 2021;10(8):1148–56.
7. Kim MH, Woo SK, Lee KC, An GI, Pandya D, Park NW, Nahm SS, Eom KD, Kim KI, Lee TS, et al. Longitudinal monitoring adipose-derived stem cell survival by PET imaging hexadecyl-4-(1)(2)(4)I-iodobenzoate in rat myocardial infarction model. Biochem Biophys Res Commun. 2015;456(1):13–9.
8. Walczak P, Wojtkiewicz J, Nowakowski A, Habich A, Holak P, Xu J, Adamiak Z, Chehade M, Pearl MS, Gailloud P, et al. Real-time MRI for precise and predictable intra-arterial stem cell delivery to the central nervous system. J Cereb Blood Flow Metab. 2017;37(7):2346–58.
9. Tachibana Y, Enmi J, Agudelo CA, Iida H, Yamaoka T. Long-term/bioinert labeling of rat mesenchymal stem cells with PVA-Gd conjugates and MRI monitoring of the labeled cell survival after intramuscular transplantation. Bioconjug Chem. 2014;25(7):1243–51.
10. Katsuoka Y, Ohta H, Fujimoto E, Izuhara L, Yokote S, Kurihara S, Yamanaka S, Tajiri S, Chikaraish T, Okano HJ, Yokoo T. Intra-arterial catheter system to repeatedly deliver mesenchymal stem cells in a rat renal failure model. Clin Exp Nephrol. 2016;20(2):169–77.
11. Wuttisarnwattana P, Gargesha M. van't Hof W, Cooke KR, Wilson DL: Automatic stem cell detection in microscopic whole mouse cryo-imaging. IEEE Trans Med Imaging. 2016;35(3):819–29.

12. El-Kersh A, El-Akabawy G, Al-Serwi RH. Transplantation of human dental pulp stem cells in streptozotocin-induced diabetic rats. Anat Sci Int. 2020;95(4):523–39.
13. Quach CH, Jung KH, Paik JY, Park JW, Lee EJ, Lee KH. Quantification of early adipose-derived stem cell survival: comparison between sodium iodide symporter and enhanced green fluorescence protein imaging. Nucl Med Biol. 2012;39(8):1251–60.
14. Puelacher WC, Mooney D, Langer R, Upton J, Vacanti JP, Vacanti CA. Design of nasoseptal cartilage replacements synthesized from biodegradable polymers and chondrocytes. Biomaterials. 1994;15(10):774–8.
15. Brun P, Abatangelo G, Radice M, Zacchi V, Guidolin D, Daga Gordini D, Cortivo R. Chondrocyte aggregation and reorganization into three-dimensional scaffolds. J Biomed Mater Res. 1999;46(3):337–46.
16. Turner NJ, Kielty CM, Walker MG, Canfield AE. A novel hyaluronan-based biomaterial (Hyaff-11) as a scaffold for endothelial cells in tissue engineered vascular grafts. Biomaterials. 2004;25(28):5955–64.
17. Naumann A, Aigner J, Staudenmaier R, Seemann M, Bruening R, Englmeier KH, Kadegge G, Pavesio A, Kastenbauer E, Berghaus A. Clinical aspects and strategy for biomaterial engineering of an auricle based on three-dimensional stereolithography. Eur Arch Otorhinolaryngol. 2003;260(10):568–75.
18. In Kim J, Kim CS. Harnessing nanotopography of PCL/collagen nanocomposite membrane and changes in cell morphology coordinated with wound healing activity. Mater Sci Eng C Mater Biol Appl. 2018;91:824–37.
19. Hartmann-Fritsch F, Biedermann T, Braziulis E, Luginbuhl J, Pontiggia L, Bottcher-Haberzeth S, van Kuppevelt TH, Faraj KA, Schiestl C, Meuli M, Reichmann E. Collagen hydrogels strengthened by biodegradable meshes are a basis for dermo-epidermal skin grafts intended to reconstitute human skin in a one-step surgical intervention. J Tissue Eng Regen Med. 2016;10(1):81–91.
20. Jiang Y, Han Y, Wang J, Lv F, Yi Z, Ke Q, Xu H. Space-oriented nanofibrous scaffold with silicon-doped amorphous calcium phosphate nanocoating for diabetic wound healing. ACS Appl Bio Mater. 2019;2(2):787–95.
21. Rosendorf J, Horakova J, Klicova M, Palek R, Cervenkova L, Kural T, Hosek P, Kriz T, Tegl V, Moulisova V, et al: Experimental fortification of intestinal anastomoses with nanofibrous materials in a large animal model. Sci Rep 2020:10(1):1134.
22. Schulz S, Angarano M, Fabritius M, Mulhaupt R, Dard M, Obrecht M, Tomakidi P, Steinberg T: Nonwoven-based gelatin/polycaprolactone membrane prove suitability in a preclinical assessment for treatment of soft tissue defects. Tissue Eng Part A 2014, 20(13-14):1935-1947
23. Uemoto Y, Taura K, Nakamura D, Xuefeng L, Nam NH, Kimura Y, Yoshino K, Fuji H, Yoh T, Nishio T, et al: Bile Duct Regeneration with an Artificial Bile Duct Made of Gelatin Hydrogel Nonwoven Fabrics. Tissue Eng Part A 2022;28(17-18):737-748
24. Cheng Y, Cheng P, Xue F, Wu KM, Jiang MJ, Ji JF, Hang CH, Wang QP: Repair of ear cartilage defects with allogenic bone marrow mesenchymal stem cells in rabbits. Cell Biochem Biophys 2014, 70(2):1137-1143.
25. Rosa S, Choi Martin, Riegler Charbalos, Pothoulakis Byung Soo, Kim David, Mooney Martin, Vacanti Joseph P, Vacanti (1998) Studies of brush border enzymes basement membrane components and electrophysiology of tissue-engineered neointestine Journal of Pediatric Surgery 33(7) 991-997 10.1016/S0022-3468(98)90520-6
26. Rotter N, Aigner J, Naumann A, Planck H, Hammer C, Burmester G, Sittinger M: Cartilage reconstruction in head and neck surgery: comparison of resorbable polymer scaffolds for tissue engineering of human septal cartilage. J Biomed Mater Res 1998;42(3):347-356.
27. Li Y, Ma T, Yang ST, Kniss DA. Thermal compression and characterization of three-dimensional nonwoven PET matrices as tissue engineering scaffolds. Biomaterials. 2001;22(6):609–18.
28. Popat KC, Daniels RH, Dubrow RS, Hardev V, Desai TA. Nanostructured surfaces for bone biotemplating applications. J Orthop Res. 2006;24(4):619–27.
29. Heath DE, Lannutti JJ, Cooper SL. Electrospun scaffold topography affects endothelial cell proliferation, metabolic activity, and morphology. J Biomed Mater Res A. 2010;94(4):1195–204.
30. Kim J, Ma T. Perfusion regulation of hMSC microenvironment and osteogenic differentiation in 3D scaffold. Biotechnol Bioeng. 2012;109(1):252–61.
31. Iijima K, Ishikawa S, Sasaki K, Hashizume M, Kawabe M, Otsuka H: Osteogenic Differentiation of Bone Marrow-Derived Mesenchymal Stem Cells in Electrospun Silica Nonwoven Fabrics. ACS Omega 2018;3(8):10180-10187. https://doi.org/10.1021/acsomega.8b01139.
32. Çetinkaya G, Türkoğlu H, Arat S, Odaman H, Onur MA, Gümüşderelioğlu M, Tümer A: LIF-immobilized nonwoven polyester fabrics for cultivation of murine embryonic stem cells. Abst J Biomed Mater Res Part A 2007;81A(4):911-919. https://doi.org/10.1002/jbm.a.31107.
33. Huber A, Pickett A, Shakesheff KM: Reconstruction of spatially orientated myotubes in vitro using electrospun parallel microfibre arrays. Eur Cell Mater. 2007;14:56-63. https://doi.org/10.22203/eCM.v014a06.
34. Matsuo Y, Morita H, Yamagishi H, Nakamura M, Takeshima Y, Nakagawa I, Imanishi J, Tsujimura T. Isolation of adipose tissue-derived stem cells by direct membrane migration and expansion for clinical application. Hum Cell. 2021;34(3):819–24.
35. Chijimatsu R, Takeda T, Tsuji S, Sasaki K, Kato K, Kojima R, Michihata N, Tsubaki T, Matui A, Watanabe M, et al. Development of hydroxyapatite-coated nonwovens for efficient isolation of somatic stem cells from adipose tissues. Regenerat Ther. 2022;21:52–61.
36. Schuurman HJ. The nude rat. Hum Exp Toxicol. 1995;14(1):122–5.
37. Fani N, Farokhi M, Azami M, Kamali A, Bakhshaiesh NL, Ebrahimi-Barough S, Ai J, Eslaminejad MB. Endothelial and osteoblast differentiation of adipose-derived mesenchymal stem cells using a cobalt-doped CaP/silk fibroin scaffold. ACS Biomater Sci Eng. 2019;5(5):2134–46.
38. Zhang H, Zhou Y, Zhang W, Wang K, Xu L, Ma H, Deng Y. Construction of vascularized tissue-engineered bone with a double-cell sheet complex. Acta Biomater. 2018;77:212–27.
39. Ojansivu M, Mishra A, Vanhatupa S, Juntunen M, Larionova A, Massera J, Miettinen S. The effect of S53P4-based borosilicate glasses and glass dissolution products on the osteogenic commitment of human adipose stem cells. PLoS ONE. 2018;13(8): e0202740.

40. Wang G, Roohani-Esfahani SI, Zhang W, Lv K, Yang G, Ding X, Zou D, Cui D, Zreiqat H, Jiang X. Effects of Sr-HT-Gahnite on osteogenesis and angiogenesis by adipose derived stem cells for critical-sized calvarial defect repair. Sci Rep. 2017;7:41135.
41. Wang Y, Wu S, Kuss MA, Streubel PN, Duan B. Effects of hydroxyapatite and hypoxia on chondrogenesis and hypertrophy in 3D bioprinted ADMSC laden constructs. ACS Biomater Sci Eng. 2017;3(5):826–35.
42. Kumbhar JV, Jadhav SH, Bodas DS, Barhanpurkar-Naik A, Wani MR, Paknikar KM, Rajwade JM. In vitro and in vivo studies of a novel bacterial cellulose-based acellular bilayer nanocomposite scaffold for the repair of osteochondral defects. Int J Nanomedicine. 2017;12:6437–59.
43. Hayrapetyan A, Bongio M, Leeuwenburgh SC, Jansen JA, van den Beucken JJ. Effect of nano-HA/collagen composite hydrogels on osteogenic behavior of mesenchymal stromal cells. Stem Cell Rev Rep. 2016;12(3):352–64.
44. Ko E, Lee JS, Kim H, Yang SY, Yang D, Yang K, Lee J, Shin J, Yang HS, Ryu W, Cho SW. Electrospun silk fibroin nanofibrous scaffolds with two-stage hydroxyapatite functionalization for enhancing the osteogenic differentiation of human adipose-derived mesenchymal stem cells. ACS Appl Mater Interfaces. 2018;10(9):7614–25.
45. Rivero G, Aldana AA, Lopez YRF, Liverani L, Boccacini AR, Bustos DM, Abraham GA. 14–3–3 epsilon protein-immobilized PCL-HA electrospun scaffolds with enhanced osteogenicity. J Mater Sci-Mater Med. 2019. https://doi.org/10.1007/s10856-019-6302-2.
46. Chuenjitkuntaworn B, Osathanon T, Nowwarote N, Supaphol P, Pavasant P. The efficacy of polycaprolactone/hydroxyapatite scaffold in combination with mesenchymal stem cells for bone tissue engineering. J Biomed Mater Res A. 2016;104(1):264–71.
47. Ramaswamy Y, Roohani I, No YJ, Madafiglio G, Chang F, Zhang F, Lu Z, Zreiqat H. Nature-inspired topographies on hydroxyapatite surfaces regulate stem cells behaviour. Bioact Mater. 2021;6(4):1107–17.
48. James AW, Levi B, Nelson ER, Peng M, Commons GW, Lee M, Wu B, Longaker MT. Deleterious effects of freezing on osteogenic differentiation of human adipose-derived stromal cells in vitro and in vivo. Stem Cells Dev. 2011;20(3):427–39.
49. Sunami H, Yokota I, Igarashi Y. Influence of the pattern size of micropatterned scaffolds on cell morphology, proliferation, migration and F-actin expression. Biomater Sci-Uk. 2014;2(3):399–409.
50. Sunami H, Yokota I, Igarashi Y. Estimation of the angles migrating cells turn on three-dimensional micro-patterned scaffolds by live cell imaging with an inverted microscope. e-J Surface Sci Nanotechnol. 2014;12:289–98.
51. Sunami H, Shimizu Y, Denda J, Yokota I, Kishimoto H, Igarashi Y. A 3D microfabricated scaffold system for unidirectional cell migration. Adv Biosyst. 2020. https://doi.org/10.1002/adbi.202000113.
52. Policha A, Zhang P, Chang L, Lamb K, Tulenko T, DiMuzio P. Endothelial differentiation of diabetic adipose-derived stem cells. J Surg Res. 2014;192(2):656–63.
53. Zhang P, Moudgill N, Hager E, Tarola N, Dimatteo C, McIlhenny S, Tulenko T, DiMuzio PJ. Endothelial differentiation of adipose-derived stem cells from elderly patients with cardiovascular disease. Stem Cells Dev. 2011;20(6):977–88.
54. Merceron C, Portron S, Masson M, Lesoeur J, Fellah BH, Gauthier O, Geffroy O, Weiss P, Guicheux J, Vinatier C. The effect of two- and three-dimensional cell culture on the chondrogenic potential of human adipose-derived mesenchymal stem cells after subcutaneous transplantation with an injectable hydrogel. Cell Transplant. 2011;20(10):1575–88.
55. Nejadnik H, Diecke S, Lenkov OD, Chapelin F, Donig J, Tong X, Derugin N, Chan RC, Gaur A, Yang F, et al. Improved approach for chondrogenic differentiation of human induced pluripotent stem cells. Stem Cell Rev. 2015;11(2):242–53.
56. Jackson WM, Aragon AB, Djouad F, Song Y, Koehler SM, Nesti LJ, Tuan RS. Mesenchymal progenitor cells derived from traumatized human muscle. J Tissue Eng Regen Med. 2009;3(2):129–38.
57. Cho H, Lee A, Kim K. The effect of serum types on chondrogenic differentiation of adipose-derived stem cells. Biomater Res. 2018;22:6.
58. Mitchell A, Ashton L, Yang XB, Goodacre R, Smith A, Kirkham J. Detection of early stage changes associated with adipogenesis using raman spectroscopy under aseptic conditions. Cytometry A. 2015;87(11):1012–9.

Publisher's Note